Journal of Research in Pharmacy

Research Article

www.jrespharm.com

Green synthesis of silver nanoparticles using *Pistacia palaestina* (Boiss). extract: Evaluation of in vivo wound healing activity

Mohammed ALSHLASH [1] *, Wassim ABDELWAHED [2], Adawia KITAZ [1]

[1] Department of Pharmacognosy and Medicinal Plants, Faculty of Pharmacy, University of Aleppo, Aleppo, Syria.
[2] Department of Pharmaceutics and Pharmaceutical Technology, Faculty of Pharmacy, University of Aleppo, Aleppo, Syria.
* Corresponding Author. E-mail: mohammedalshlash994@gmail.com (M.A.); Tel. +963991607908

Received: 17 November 2022 / Revised: 24 December 2022 / Accepted: 29 December 2022

ABSTRACT: This paper conducts green synthesis of silver nanoparticles using *Pistacia palaestina* fruit extract and studies the effects of the fabrication conditions on the size of fabricated nanoparticles during the synthesis process and the evaluation of its wound healing activity *in vivo*. Methods: *P. palaestina* extract has been used to reduce silver nitrate solution to AgNPs. The synthesized AgNPs were characterized using UV-Vis spectroscopy, Dynamic Light Scattering (DLS), Atomic Force Microscopy (AFM), and Scanning Electron Microscopy (SEM). The fabricated AgNPs were prepared as an ointment (1% w/w) and evaluated for wound healing activity using an incision wound model on rats. The time of healing was determined and compared with a positive control (gentamicin ointment 0.1%) and a negative control. Results: The fabricated AgNPs have a dark brown color, and their absorption peak was at 430 nm. The obtained particles have an average diameter of 36 nm by SEM, 55.64 nm by DLS, and 100 nm by AFM. AFM and SEM images confirmed the spherical shape of prepared AgNPs. The optimal formula for preparing AgNPs was by using fruit extract (pH 7) at a ratio of (1:9) at 35°C for 24 h. The prepared AgNPs ointment (1%) accelerated wound healing compared to a negative control group, as the time of healing was 9 ± 1.41, 12 ± 1.73, and 17 ± 2.00 days, respectively. Conclusion: It is concluded that *P. palaestina* extract can be utilized for fabricating AgNPs without any additions, and they have wound healing effect in experimental rats.

KEYWORDS: *Pistacia palaestina*; Silver nanoparticles; Green synthesis; Wound healing; Dynamic Light Scattering.

1. INTRODUCTION

Nanotechnology is an important field of modern research, and it has started to appear as a new science. It studies dimensions of particles between 1 and 100 nanometers [1]. In this size range, particles have chemical and physical new properties that can be applied in many scientific fields like pharmacy, medicine, cosmetics formulation, optics, gene therapy, detection of genetic disorders, and data storage [2-4]. There are many categories to classify nanoparticles (NPs) depending on their size, shape, and physical and chemical properties which include: carbon-based NPs, metal NPs, polymeric NPs, and lipid-based NPs [5].

Among the metal nanoparticles, silver nanoparticles (AgNPs) were the subject of significant recent interest because of their distinctive nature and unique characteristics such as optical, electrical, catalysis, and antibacterial properties [6]. These characteristics have been used in the biomedical field for drug delivery, diagnostics, pharmacology, wound dressings, molecular imaging, antifungal, and as preventing agents of infection in wounds and burns [2,7].

There are several approaches to synthesizing AgNPs as follows: (1) The chemical method is more diverse, mainly including the chemical reduction approach. Usually, some stabilizer agents and reduction dispersants are used in this approach, like sodium borohydride, ascorbic acid, and sodium citrate [8-9]. (2) The biological method is important, where the aqueous solution of silver nitrate is reduced to AgNPs by bacteria, plants, and yeasts [10]. (3) The physical method generally uses mechanical grinding, laser burning, and gas phase deposition to synthesize nanoparticles with the benefits of easier standards and higher purity. However, the particles' dimensions in this method are larger than the dimensions in the chemical and biological methods [10]. The chemical method is utilized to fabricate AgNPs, but it is expensive and needs to use toxic and non-

How to cite this article: Alshlash M, Abdelwahed W, Kitaz A. Green synthesis of silver nanoparticles using *Pistacia palaestina* (Boiss). extract: Evaluation of in vivo wound healing activity. J Res Pharm. 2023; 27(3): 1170-1187.

ISSN: 2630-6344

http://dx.doi.org/10.29228/jrp.407

ecofriendly solvents [8,10]. The approaches based on bacteria are not industrially possible because they need highly sterile conditions and preservation [11]. Moreover, the formation rate is slow and only a limited number of shapes and sizes are malleable compared to approaches involving plant materials. Therefore, using plant extracts is more effective than using bacteria because there is no need for special preparation for culture and isolation techniques.

Furthermore, green synthesis is eco-friendly and safe and uses biocompatible agents for the synthesis of silver nanoparticles compared with chemical and physical methods [12,13]. Plant extracts contain many biomolecules such as terpenoids, flavonoids, phenolic acids, carbohydrates, proteins, and enzymes, where these biomolecules contribute to the bio-reduction of silver ions to metal nanoparticles and play an important function in the coating of synthesized nanoparticles [14]. The biological method for the formation of AgNPs is based on reducing agents such as fungi, bacteria, and plant extracts, which interact with silver ions and reduce them into silver-NPs. Many researches have been stated on the fabrication of AgNPs by plant extracts such as *Drosera binata*, *Cassia roxburghii* (Leaves), *Bryonia laciniosa* (Leaves), *Naringi crenulata* (Leaves), and *Aloe vera* (Leaves) [15-18].

One of the most usages of AgNPs is in aiding the wound healing process at a high rate. Because of their impacts are as an antimicrobial or as an antioxidant compounds. Wound healing is an essential, regulated and intricate sequence of several cellular and biochemical phenomena to recover the integrity of the skin [15]. Normal healing is a process that consists of three phases: Inflammation, proliferation, and maturation [19].

The genus *Pistacia* belongs to the Anacardiaceae family which contains about 70 genera and more than 600 species. The species of this genus are evergreen or deciduous shrubs and trees with well-developed vertical resin canals, which are growing to 8–10 meters tall. They are widespread in central Asia and the Mediterranean basin [20]. *Pistacia palaestina* is used in folk medicines to treat eczema, cough, gastrointestinal diseases (anti-helicobacter), kidney stones, and hypertension. *P. palaestina* has antioxidant, antimicrobial, and antifungal activities. Also, *P. palaestina* methanolic extract was reported for its antimicrobial activity on *Escherichia coli* bacteria. Furthermore, it supports in the protection of the blood vessels and the liver by preventing the Low-density lipoproteins LDL oxidation [21]. It has been reported that *P. palaestina* contains many phytochemical compounds, including phenolic compounds, flavonoids, and tannins [22]. Existing literature reports successful synthesis of AgNPs through a green method where the capping and reducing agent selected was the aerial parts of *Pistacia* species. For example, in a previous paper, *Pistacia terebinthus* methanolic extract was used to synthesis AgNPs using a green method [23]. In another paper, *Pistacia atlantica* leaf extract was used to production AgNPs, where it was as a reductant, capping, and stabilizer agent [24]. Also, in a previous research, *Pistacia lentiscus* leaves extract was utilized to fabricate silver nanoparticles and these nanoparticles showed antimicrobial a good activity against bacterial and fungal [25].

The choice of *Pistacia palaestina* fruits (see Figure 1) was done because of its the presence of important functional groups (see Figure 2) and benign nature lets AgNPs to be stable and prevents the agglomeration of nanoparticles, too. Yet to the best of our knowledge no study found in the literature have reported the use of *P. palaestina* fruits in green synthesis of silver nanoparticles. This study aims to synthesize AgNPs using the fruit extract of *P. palaestina* and to investigate the effect of pH, temperature, a quantity of plant extract (ratio), and reaction time on the synthesis process. The produced AgNPs were characterized by Ultraviolet-Visible (UV-vis) spectroscopy, Fourier Transform Infrared (FTIR) spectroscopy, Atomic Force Microscopy (AFM), Dynamic Light Scattering (DLS), Zeta Potential measurements (ZP), and Scanning Electron Microscopy (SEM). The wound-healing activity of the synthesized AgNPs was tested on experimental rats using an incision wound model.

Journal of Research in Pharmacy
Research Article

Figure 1. Photograph of *Pistacia palaestina* fruits.

http://dx.doi.org/10.29228/jrp.407
J Res Pharm 2023; 27(3): 1170-1187

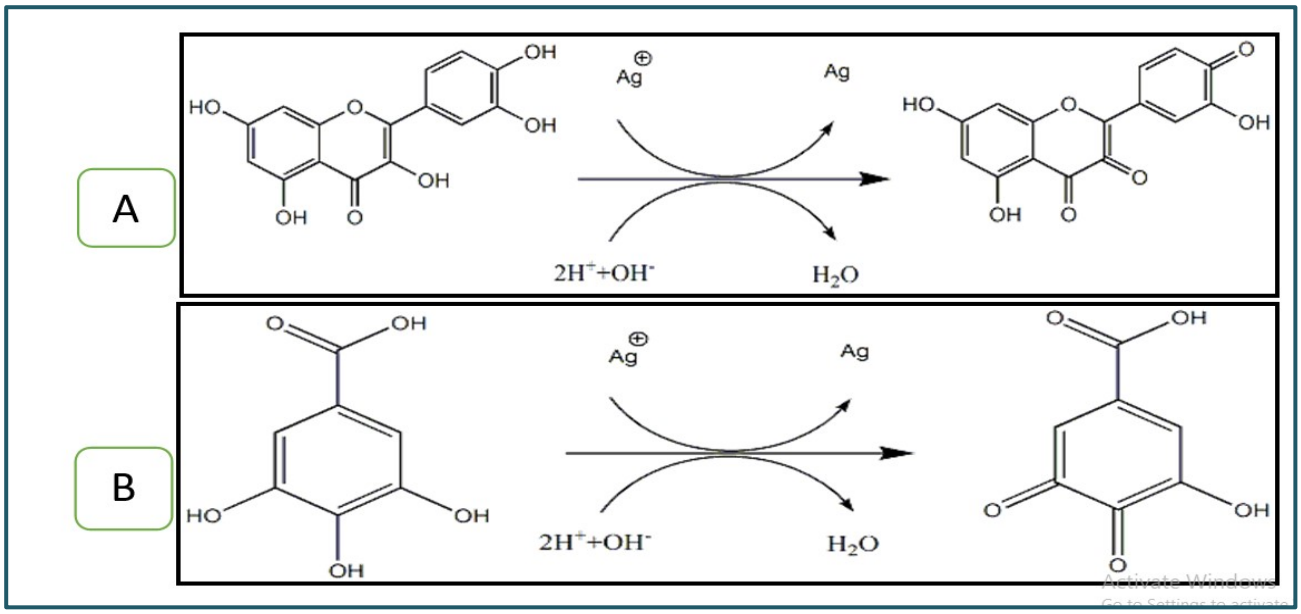

Figure 2. Possible reduction mechanism of Ag^+ ions to AgNPs by (A) flavonols and (B) gallic acid (the main phytochemicals in plant extracts).

2. RESULTS and DISCUSSION

2.1. Studying the factors affecting AgNPs size during synthesis process

2.1.1. pH value

The effect of pH value on the size of silver nanoparticles is shown in Table 1. It is observed that the particle size was 60.24 nm with polydisperse index (PDI) 0.441 when using pH 4.65. However, the particle size increased dramatically to 365.2 nm when using pH 11 and the sample was highly polydispersed (PDI = 0.678). Finally, the particle size was 59.24 nm with PDI (0.192) at pH 7, thus, pH 7 was considered the preferred value during silver nanoparticle synthesis. According to the literature, many biomolecules in plant extracts have an electrical charge which could be affected by pH. These biomolecules play an important role in stabilizing NPs and any change of their electrical charge may cause a modification in the size of AgNPs. When the pH is high, the amount of H^+ ions in the solution is low, leading to a fast split of solution particles and simultaneous reduction of a large number of silver ions, leading to the creation of many nuclei. As a result, the amount of reduced ions decreases, and the growth of AgNPs increases. On the other hand, at neutral pH, the amount of H^+ ions in the solution is appropriate and this lets the available amount of Ag ions to be reduced so that some of the nuclei have enough time to develop into spherical nanoparticles [26].

On the other hand, from Table 1, It is observed that the ZP value was -20.00 millivolt (mV) when using pH 4.65, and the ZP was -20.90 mV when using pH 7. Also, the ZP value increased clearly to -34.70 mV when using pH 11. This negative potential value could be due to the capping of polyphenolic and proteins constituents present in the plant extracts. Also, the changes in pH can cause an increase in ionization of polyphenolic in the plant extract, and this may modify the double-layer properties that can affect the zeta potential of the formula [26].

Table 1. Effect of pH on silver nanoparticles size.

Extract volume mL	silver nitrates volume mL	silver nitrate: extract ratio	Temperature ˚C	stirring time h	**pH**	Z-Average (nm)	PDI	Zeta potintioal (mV)
10	90	1:9	25	24	**4.65**	60.53 ± 6.83	0.441 ± 0.027*	-20.0 ± 1.1
10	90	1:9	25	24	**7**	59.24 ± 10.12	0.192 ± 0.02*	-20.9 ± 0.9
10	90	1:9	25	24	**11**	365.2 ± 3.42+	0.678 ± 0.085*	-34.7 ± 1.5

Data are mean (n = 3) ± SD (n = 3, p < 0.05). d-nm: diameter-nm, PDI: Polydisperse index.

*Express the presence of a significant difference between all means (PDI) at significant differences at (P < 0.05).

+Express the presence of a significant difference between all means (Z-Average) at significant differences at (P < 0.05).

2.1.2. Reaction temperature

The effect of temperature on the size of manufactured silver nanoparticles was shown in Table 2. A dark brown color appeared directly at high temperatures of 70 °C where the size was (54.53) nm. In addition, a brown color arose after 24 h, at temperatures of 25 °C and 35 °C where the size was 59.24 nm and 51.29 nm, respectively. According to the literature, reaction temperature has an important effect on the process of synthesis of AgNPs. Usually, the reaction takes a long time (at 25 °C) to complete, but the reaction can be accelerated by increasing the temperature because it stimulates the phytochemical compounds in plant extracts which leads to a fast reduction of Ag^+ ions to Ag^0 [27,28].

Table 2. Effect of temperature on silver nanoparticles size.

Extract volume mL	silver nitrates volume mL	silver nitrate: extract ratio	**Temperature ˚C**	stirring time h	pH	Z-Average (d-nm)	PDI	Zeta potintioal (mV)
10	90	1:9	**25**	24	7	59.24 ± 10.12	0.192 ± 0.02*	-20.9 ± 0.9
10	90	1:9	**35**	24	7	51.29 ± 4.07	0.365 ± 0.015*	-21.4 ± 1.1
10	90	1:9	**70**	24	7	54.53 ± 4.96	0.291 ± 0.014*	–

Data are mean (n = 3) ± SD (n = 3, p < 0.05). d-nm: diameter-nm, PDI: Polydisperse index.

*Express the presence of a significant difference between all means (PDI) at significant differences at (P < 0.05).

+Express the presence of a significant difference between all means (Z-Average) at significant differences at (P < 0.05).

2.1.3. The silver nitrate: plant extract ratio

The effect of the ratio (silver nitrate: plant extract) on the size of manufactured silver nanoparticles is shown in Table 3. The optimal ratio (extract solution: silver nitrate) to create AgNPs was (1:9), where this ratio produced a particle size (51.29) nm with low PDI (0.365). Comparing these results with the literature, increasing the amount of plant extract leads to an increase in the reduction compounds, thus this extract may increase the creation of silver nanoparticles with a high possibility of agglomeration later [1].

Table 3. Effect of the ratio (plant extract: silver nitrate solution) on silver nanoparticles size.

Extract volume mL	silver nitrates volume mL	**silver nitrate: extract ratio**	Temperature ˚C	stirring time h	pH	Z-Average (d-nm)	PDI	Zeta potintioal (mV)
20	80	**2:8**	35	24	7	76.9 ± 7.92^{+}	0.457 ± 0.016*	–
10	90	**1:9**	35	24	7	51.29 ± 4.07	0.365 ± 0.015*	-21.4 ± 1.1
5	95	**0.5:9.5**	35	24	7	36.33 ± 7.64	0.636 ± 0.042*	–

Data are mean (n = 3) ± SD (n = 3, p < 0.05). d-nm: diameter-nm, PDI: Polydisperse index.

*Express the presence of a significant difference between all means (PDI) at significant differences at (P < 0.05).

+Express the presence of a significant difference between all means (Z-Average) at significant differences at (P < 0.05).

2.1.4. Reaction stirring time

Table 4 displays the mean nanoparticles size of the mixture of *P. palaestina* fruit extract and silver nitrate solution (1 mmoL/L) as a function of time (6 and 24 hours). From Table 4, it was observed that the particle size decreased with the increase in the reaction stirring time. Thus, the optimal stirring time for the completion of the reaction in this study was 24 h. However, the rapid formation of AgNPs indicates the good reducibility and interaction between the phytochemical components in the *P. palaestina* fruits extract and silver nitrate solution, which plays an important role in stabilizing nanoparticles (AgNPs) produced in the medium [1,27].

Table 4. Effect of reaction straining time on silver nanoparticles size.

Extract volume mL	silver nitrates volume mL	silver nitrate: extract ratio	Temperature ˚C	pH	**stirring time h**	Z-Average (d-nm)	PDI	Zeta potintioal (mV)
10	90	1:9	35	7	**6**	66.9 ± 5.37	0.257 ± 0.02*	–
					24	51.29 ± 4.07	0.365 ± 0.015*	-21.4 ± 1.1
20	80	2:8	25	7	**6**	47.35 ± 7.28	0.220 ± 0.02*	–
					24	36.33 ± 7.64	0.636 ± 0.08*	–
20	80	2:8	25	7	**6**	67.32 ± 7.58	0.314 ± 0.03*	–
					24	57.49 ± 5.27	0.123 ± 0.02*	–

Data are mean (n = 3) ± SD (n = 3, p < 0.05). d-nm: diameter-nm, PDI: Polydisperse index.

*Express the presence of a significant difference between all means (PDI) at significant differences at (P < 0.05).

+Express the presence of a significant difference between all means (Z-Average) at significant differences at (P < 0.05).

2.1.5. Optimal formula parameters

According to the results of this study, it is concluded that the optimal formula and parameters for producing silver nanoparticles use fruit extract in 9:1 ratio (silver nitrate: extract) at 35 °C for 24 h and pH 7. This formula has been selected for later characterization, stability study, and animal experiments.

2.2. Characterization of silver nanoparticles

2.2.1. Ultraviolet-Visible (UV–Vis) spectroscopy

In this study, the $AgNO_3$ solution was colorless and after 6 h of adding plant extract, a yellow color appeared, affirming the formation of AgNPs, as shown in Figure 3. The strength of the color increased after 24 h indicating a progress in NP concentration [29]. Several studies on the preparation of AgNPs from plant extracts confirmed that, when mixing extracts with the $AgNO_3$ solution, the color changed to brown, confirming the production of AgNPs [4,6,13]. The UV–Vis spectrum of silver nanoparticles synthesized using

P. palaestina fruits is shown in Figure 4. The results showed absorption bonds at around 430 nm. It seemed that AgNPs straight originate from the π-π*electron, where the silver nanoparticles' free electrons influence the Surface Plasmon Resonance (SPR) and absorption frequencies. Several previous works have shown that the SPR between 400 and 450 nm have observed the existence of AgNPs [25,23]. Many researchers have showed that the production of the SPR peak is controlled by several factors including the shape and size of particles [30,31]. Compared to previous papers, our findings were similar to that a study by Naghmachi et al., 2022, when using *Pistacia terebinthus* extract to formation silver nanoparticles, the peak of absorption was around at 420-430 nm [23].

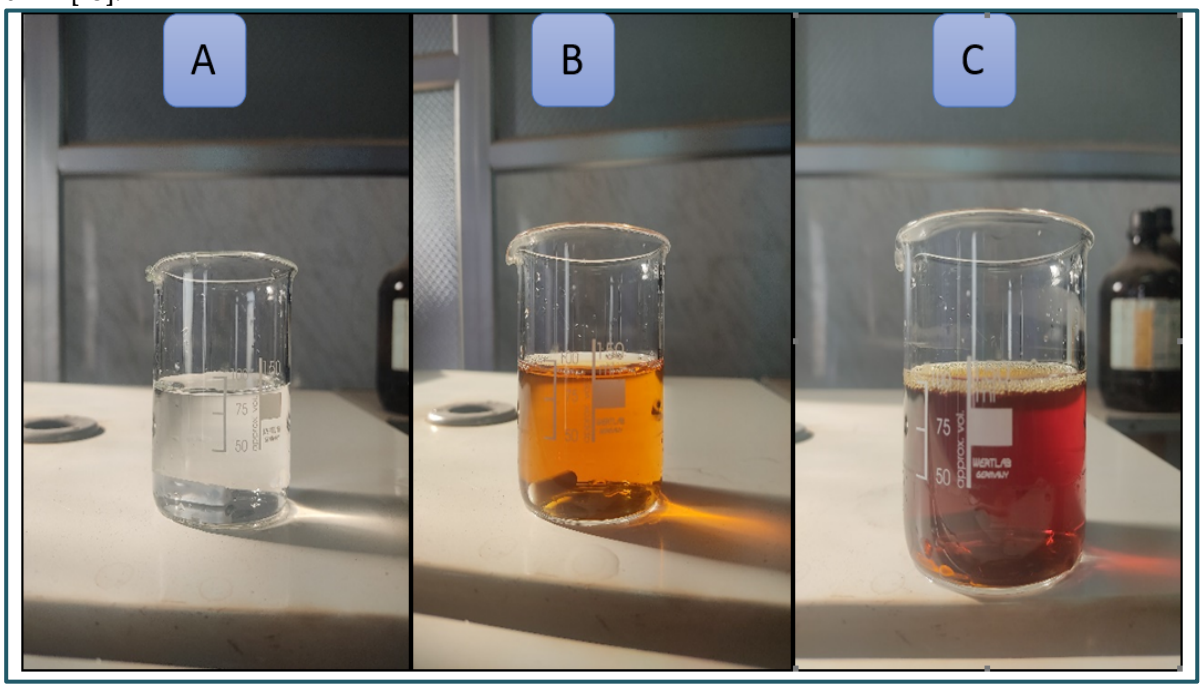

Figure 3. Visual appearance of the silver nanoparticles suspension formed using *Pistacia palaestina* (A) zero hours, (B) 6 hours and (C) 24 hours.

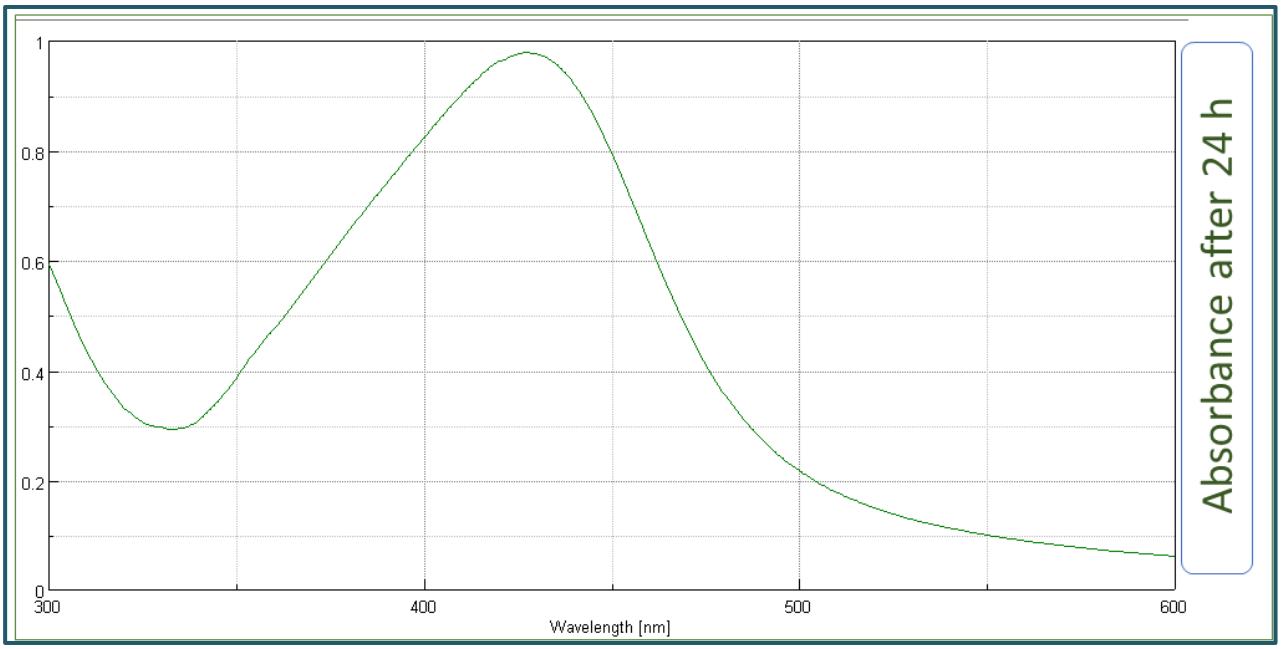

Figure 4. UV-Vis spectrum of synthesized silver nanoparticles using *Pistacia palaestina* fruits.

2.2.2. FTIR spectroscopy

The FTIR measurement was carried out to detect the active biomolecules that could contribute to the reduction (Ag^+ ions to Ag^0), capping, and stabilization of the synthesized silver nanoparticles [31,24]. The FTIR spectrum of silver nanoparticles synthesized using *P. palaestina* fruits is presented in Figure 5. The adsorption bands at 3388 cm^{-1} (O-H stretch) [32]; 2925 cm^{-1} and 2855 cm^{-1} (C-H stretch of saturated alkanes) [33]; 1613 cm^{-1} (-C=O stretch) [32]; 1395 cm^{-1} (a geminal methyl group stretch) [32]; 1072 cm^{-1} (C-O-C stretch) [33]; 825cm^{-1} and 766cm^{-1} (aromatic compounds stretch) were observed [34]. Besides, FTIR analysis verified the chemical connection and different functional groups of the prepareded AgNPs [23]. According to literature reports, hydroxyl, carbonyl, and amide groups in polyphenols, flavonoids, proteins, and other biomolecules could reduce Ag^+ ions to AgNPs. Moreover, many hydroxyl groups could make complexes with silver on the surface of nanoparticles, causing their stabilization and capping [33].

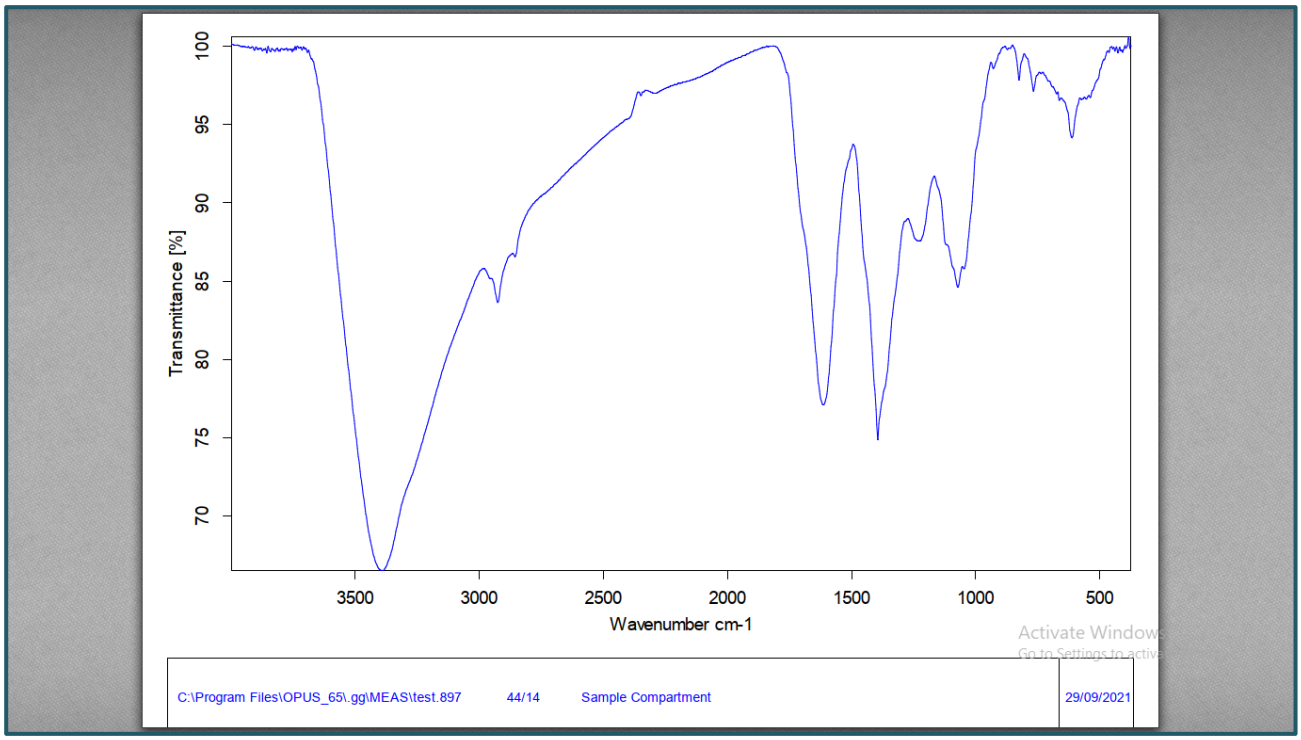

Figure 5. FTIR spectrum of the synthesized silver nanoparticles prepared using *Pistacia palaestina* fruits.

2.2.3. Dynamic Light Scattering (DLS) and Zeta Potential measurements (ZP)

The particle dimension of the synthesized silver nanoparticles is measured by using the dynamic light scattering (DLS) technique. DLS is a unique technique for describing the size of suspension dispersions which use the lighting of a suspension of molecules or particles undergoing Brownian movement by a laser ray [35]. The particle size of optimal biosynthesized silver nanoparticles is presented in Figure 6. It is shown that the size distribution of AgNPs varied from 10 to 110 nm and the Z-average of the produced silver nanoparticles was 27.82 r-nm (radius-nm), or 55.64 d-nm (diameter-nm) and PDI was 0.289. Comparing the works of literature, the findings in this study differ from other papers. For instance, *Pistacia lentiscus* leaves extract was used to produce silver nanoparticles with a size range of 24-26 nm [25]. In another study, *Pistacia atlantica* leaves extract was used to form silver nanoparticles with particle sizes between 17-18 nm [24]. The zeta potential of the synthesized AgNPs was -21.4 mV. It is concluded that the surface of the produced AgNPs is negatively charged in the medium. The negative charge causes repulsion forces between the particles and confirms that AgNPs are stable (see capture 2.3). According to the literature, the ZP value could be negative or positive; the negative value shown by AgNPs may be due to the possible capping of the phytochemical components (polyphenols and proteins) present in the plant extracts [30,31,48]. These results are supported by FTIR analysis which refers to the presence of polyphenols and proteins in the plant extract.

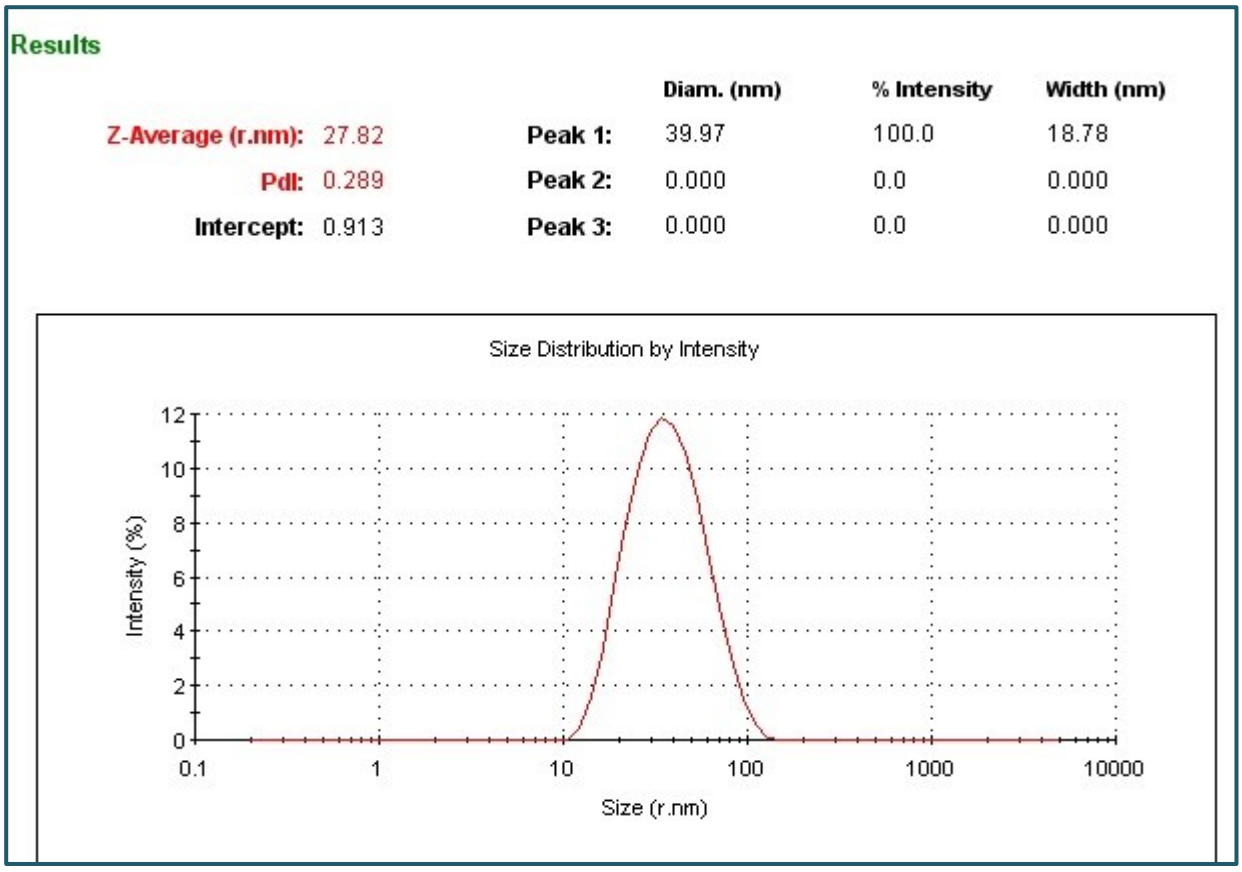

Figure 6. Size distribution measurement of produced AgNPs was determined by DLS technic.

2.2.4. Atomic force microscopy (AFM) analysis

The AFM study is carried out in order to observe the surface and morphology of AgNPs. In addition, it images the individual particle and is useful to measure its dimensions [32]. The synthesized silver nanoparticles were characterized by AFM analysis. The 3D and 2D topographic photograph features of synthesized AgNPs from *P. palaestina* fruit extract are shown in Figure 7. The results revealed the presence of spherical-shaped AgNPs with an average particle size (Z-average) of 100 nm diameter (see Figure 7-C). Our findings are in accordance with previous reports of AgNPs produced from several plant species [49,36]. On the other hand, the results (Z-average) in AFM differed from the Z–average in DLS, which may be due to the "tip broadening effect" resulting from the larger radius of curvature at the end of the tip interacting with the sample [37].

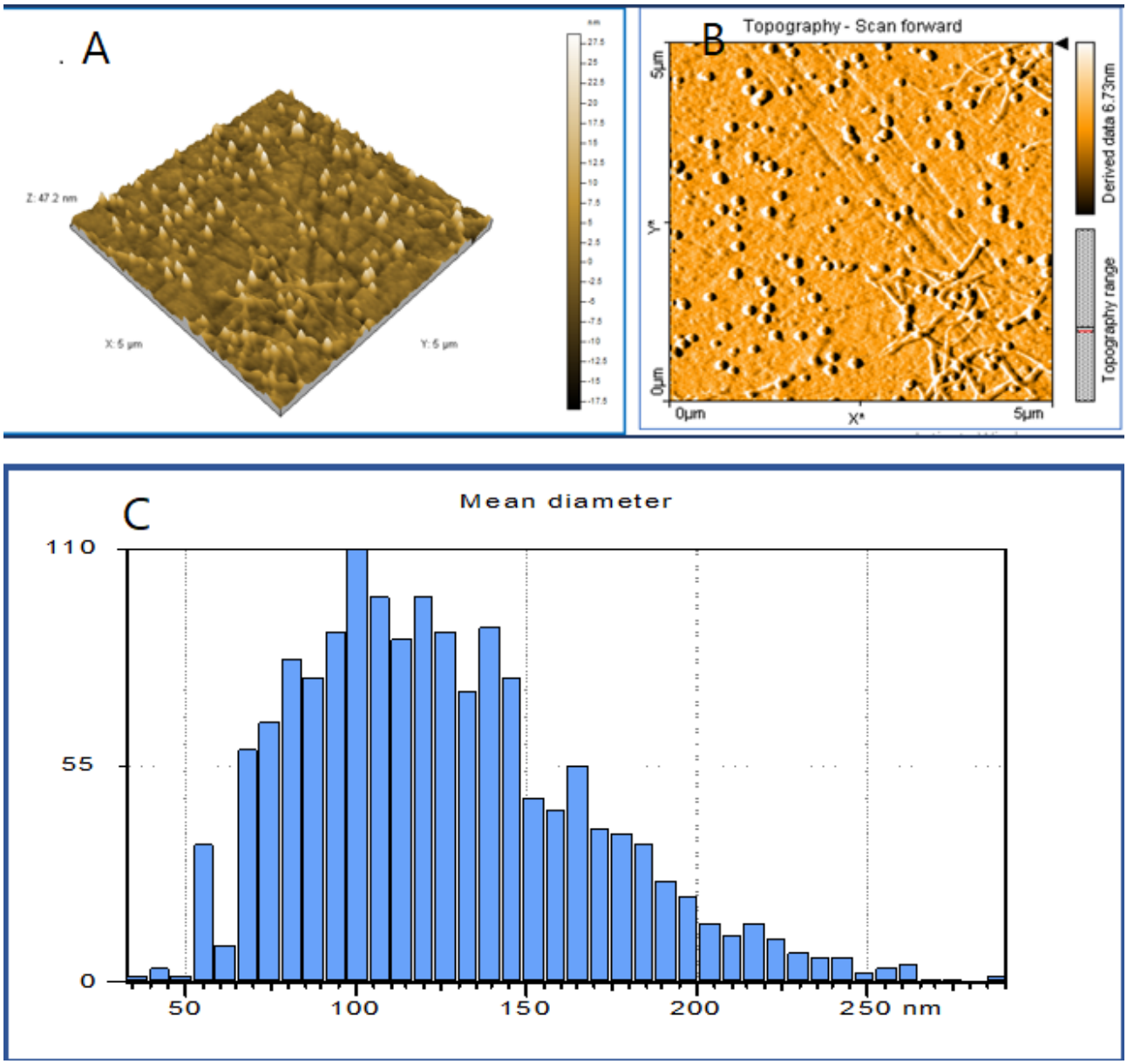

Figure 7. Atomic force microscopy (AFM) images of the formed AgNPs (A) 3D images, (B) 2D images, and (C) mean diameter.

2.2.5. Scanning Electron Microscope (SEM)

The particle size and morphology of silver nanoparticles were studied by using SEM analysis [49]. The SEM image of synthesized AgNPs from *P. palaestina* fruits extract showed that the particles were spherical in shape with the range of 21-64 nm in diameter and the average size was 36 nm diameter, as shown in Figure 8. In addition, there was no observed agglomeration or aggregation between the particles. According to the literature, the shapes and sizes of metal nanoparticles are influenced by several factors, including time of incubation, pH, method of preparation, as well as temperature [38]. However, results found from DLS and SEM may tend to differ because both of the methods are based on different techniques of characterization and the sample preparation methods are completely different, too. Comparing the works of literature, the findings in this paper similar to other papers. For instance, *Pistacia terebinthus extract* was utilized to form silver nanoparticles with a size of 32 nm diameter and had spherical shape [23].

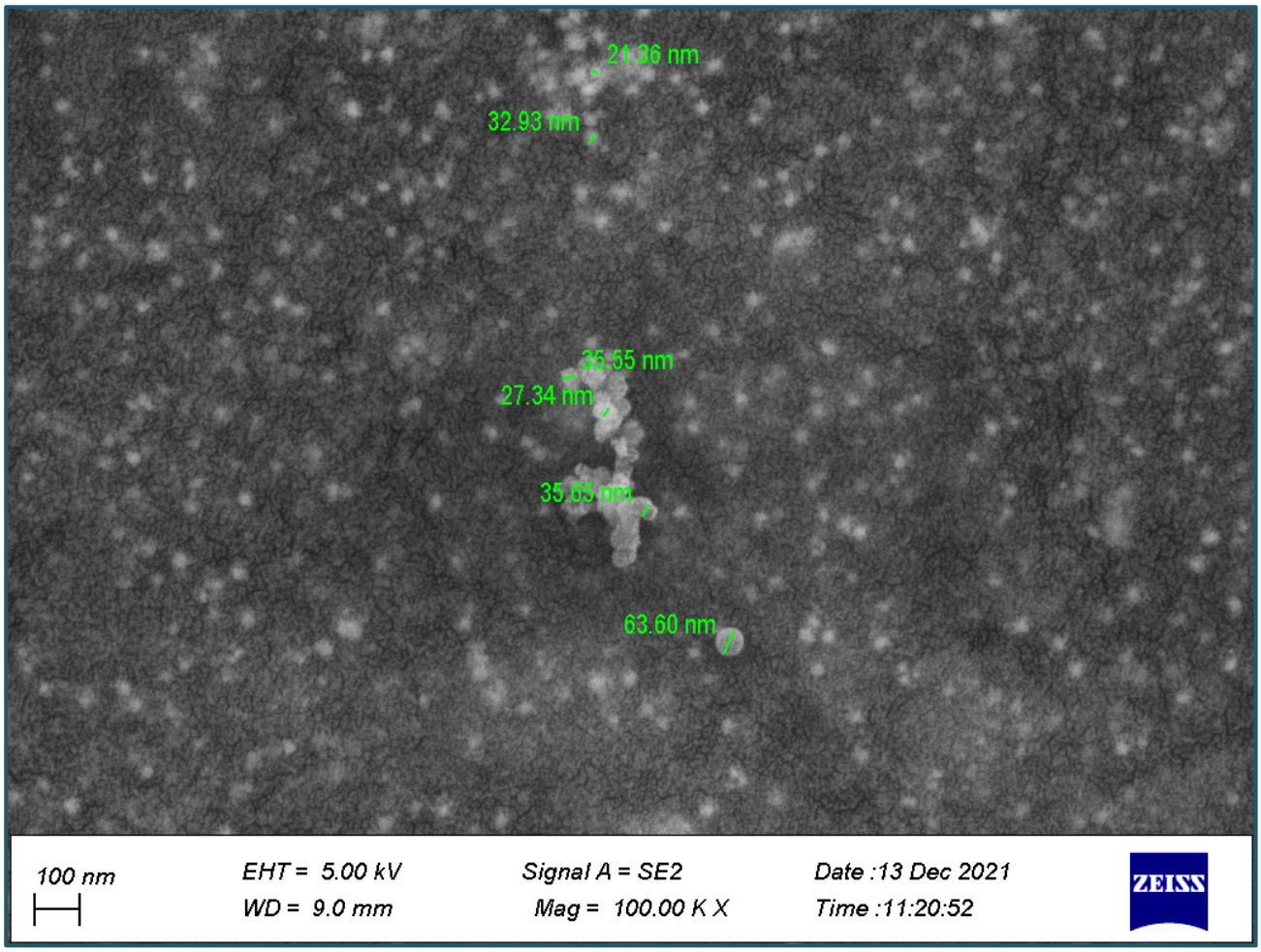

Figure 8. Image of scanning electron microscope (SEM) of silver nanoparticles produced by *Pistacia palaestina* fruits extract.

2.3. Stability of the synthesized silver nanoparticles after 60 days

The synthesized silver nanoparticles were stored at a temperature of 8 °C and the effect of this on the particle size was monitored as presented in Table 5. From the table, it is concluded that: no significant changes in particle size were observed during ten days. Moreover, storage for short periods (30 and 45 days) increased the particle size slightly from 51.21 to 59.02, and 72.96 nm respectively. Later, storage for a period of 60 days increased the particle size to 84.78 nm. However, the prepared AgNPs remained within the accepted nanoscale (smaller than 100 nm). These results correspond with the result of zeta potential measurement, which reflects electrostatic repulsion between particles and prevents their aggregation later [39]. Nonetheless, it is not easy to find studies in the literature which estimate the stability of Ag NPs for extended periods of time. Besides, most of the researchers report that particles are steady for only a short period of time without agglomeration [40,13].

Table 5. Effect of the storage period on silver nanoparticles size.

Duration Days	Z-Average size(d-nm)	PDI
1	51.29 ± 4.07 *	0.365 ± 0.015
10	51.21 ± 5.67	0.388 ± 0.02
30	59.02 ± 5.72	0.526 ± 0.04
45	72.96 ± 2.77 *	0.265 ± 0.02
60	84.78 ± 3.73 *	0.470 ± 0.03

Data are mean (n = 3) ± SD (n = 3, $p < 0.05$). d-nm: diameter-nm, PDI: Polydisperse index.

*Express the presence of a significant difference with the Z-Average (51.21 d-nm) at significant differences at ($P < 0.05$).

2.4. Evaluation of Wound Healing Activity

After conducting wound incision, the ointments were applied topically on rats. Neither changes in rats' behavior nor their death were observed during 24 days (the experimental period). In the incision wound model, prepared AgNPs ointment-treated rats showed significant contraction in the wound area and faster healing of the wound (9 ± 1.41 days), which is more similar to the values of the gentamicin ointment-treated rats (12 ± 1.73 days) as well as the group IV (negative control) had slow healing of the wound (17 ± 2.00). But, the untreated rats' group had slower healing of the wound (more than 21). The present study showed that the prepared AgNPs at concentration (1% w/w) in the ointment base was potent to produce significant wound healing activity in rats using an incision wound model. In addition, AgNPs-treated rats revealed better wound healing activity compared with that of either positive or negative-control groups. The percentage of wound contraction and mean time of healing for all groups are shown in Table 6.

Table 6. Effects of synthesized AgNPs ointment on an incision wound model.

Post wounding days	Wound area (mm^2)			
	Group I without treatment	Group II Gentamicin ointment	Group III AgNPs ointment	Group IV The ointment base
0	00 ± 00	00 ± 00	00 ± 00	00 ± 00
3rd	12.6 ± 1.73	17.53 ± 5.42	28 ± 3.44	10.04 ± 1.94
6th	28.26 ± 5.11	43.13 ± 6.67	66 ± 6.12	28.07 ± 2.6
9th	37.93 ± 6.35	65.2 ± 5.22	**100**	39.9 ± 4.97
12th	46.73 ± 5.85	**100**	-	59.53 ±3.74
15th	57.73 ± 4.76	-	-	77.93 ± 2.36
18th	69.4 ± 2.47	-	-	**100**
21st	75.67 ± 6.32	-	-	-
24th	**100**	-	-	-
Period of healing (days)	**23 ± 2.55 ***	**12 ± 1.73 ***	**9 ± 1.41 ***	**17 ± 2.00 ***

* Express the presence of a significant difference with all groups at Significant differences at ($P < 0.05$).

Note: Values are expressed as mean ± SD, n = 5 rats in each group, $P < 0.05$ is significant when compared to the Group I (without treatment). The percentage of wound contraction is given in parentheses.

The improved wound contraction might be due to the minimized bacterial count and decreasing lymphocytes in the infected wound site, which can consequently restore tissue integrity and often results in satisfactory healing of damaged sites [41]. Also, the biosynthesized AgNPs showed good effects through the reduction in inflammation and completely re-epithelialized the epidermis and downregulating the level of pro-inflammatory cytokines such as interleukin (IL)-1β, IL-6, and tumor necrosis factor-alpha (TNF-α) in the infected wound site [14]. Similarly, Saraschandra Naraginti et al. investigated the effect of the biosynthesized AgNPs in epidermal reepithelialization and dermal contraction through wound healing and concluded that biosynthesized AgNPs could increase the rate of wound contraction [42]. This property could be explained through the promotion of the production and migration of keratinocytes [43]. In addition, biosynthesized AgNPs could increase the differentiation of fibroblasts into myofibroblasts, thus inducing wound closer [44].

3. CONCLUSION

In the current work reported, silver nanoparticles have been produced successfully by using *Pistacia palaestina* which is described as an economical, eco-friendly, and more effective method than chemical and physical methods. The synthesized AgNPs were characterized by UV-vis, FT-IR, AFM, DLS, and SEM analyses. FTIR spectrum revealed the presence of phytochemicals in *P. palaestina* extract which helped bio-reduction. From SEM analysis, we concluded that the prepared AgNPs have a spherical shape with an average size of 36 nm. Also, the biosynthesized AgNPs is stable even for up to 60 days. Furthermore, the biosynthesized AgNPs accelerated wound healing compared to a control group and standard drug (gentamicin 0.1 %) in rats. Hence, due to their stable and benign nature and wound-healing property, these AgNPs may be used for remedial and industrial purposes in the future. Nevertheless, the utilization of AgNPs needs more detailed research on several issues such as its activities at the cellular and molecular levels.

4. MATERIALS AND METHODS

4.1. Chemicals, Equipment, and Plant materials

Chemicals: Silver nitrates 99.99% purchased from Sigma-Aldrich, Methanol 99% (Eurolab, UK), Sodium hydroxide 98% (Medex, UK), Ethanol GR (Eurolab, UK), Distilled deionized water (d.H2O).

Equipment: Ultrasonic bath (POWERSONIC 405, Hwashin Technology Co., Korea), Sensitive balance (Sartorius TE214, Germany), UV-1800 spectrophotometer (Shimadzu, Japan), Rotary evaporator (Heidolph Instruments, Germany), Ultrapure TM water purification system (Lotun Co., Ltd., Taipei, Taiwan), Crison pH meter model TitroMatic 1S, Zetasizer instrument (DLS; Zeta-size Nano-ZS; Malvern Instruments, UK).

Plant materials**:** Fresh fruits (see Figure 1) of *P. palaestina* were collected in August 2021 from wild plants growing in the Aleppo region (36° 12' 0" N - 37° 36' 0" E, Aleppo, north of Syria). It was authenticated by an expert at the Faculty of the Agriculture University of Aleppo, Syria. The fruits were cleaned of dust, washed, and dried in shade for ten days. Then, the dried fruits were crushed to obtain a suitable fine powder, and subsequently, they were packaged in opaque and airtight containers until later use.

4.2. Preparation of *P. palaestina* extract

The dry fruits of *P. palaestina* (5 g) were extracted with 100 mL of methanol (60%) through an ultrasonic bath, three times at 40 °C for one hour. The samples were filtered using filter paper (Whatman's NO1) and evaporated to a volume of 100 mL by using rotary evaporator apparatus. After that, it was kept in a refrigerator at 8°C and then used later for the synthesis of silver nanoparticles [45].

4.3. Green synthesis of silver nanoparticles

For the synthesis of silver nanoparticles, 10 mL of the previous extract is dropped into an Erlenmeyer flask containing 90 mL of silver nitrate solution ($AgNO_3$ 1mmoL/L) and is stirred continuously at 35 °C for 24 h. During the synthesis process, silver ions (Ag^+) are reduced to Ag^0 nanoparticles by phytochemical compounds (see Figure 2) in the extract, which is observed based on the color change of the reaction mixture from colorless to light yellow and then intense dark brown, which confirms the formation of the silver nanoparticles in the solution [46,47].

4.4. Studying the factors affecting the size of AgNPs during synthesis process

Effects of four important parameters (experimental factors) which are pH, reaction temperature, volume ratio, and reaction stirring time on the formation of AgNPs were carried out and the size of the nanoparticles was examined using a Zetasizer instrument.

pH: The fruit extract had an initial pH of 4.5. With the help of alkali (1 N NaOH solution), different pH (4.5, 7, and 11) was adjusted and measured using a pH meter (Crison pH meter model TitroMatic 1S) [48].

Reaction temperature: AgNPs were synthesized at different temperatures 25, 35, and 70 ^{0}C [49].

The ratio of plant extracts to silver nitrate solution (V/V): The general variable in determining the shape and size of AgNPs is the ratio of plant extract to silver nitrate solution. The ratio has been studied at different values as follows (plant extract/silver nitrate), (20:80), (10:90), (5:95) [50].

Reaction stirring time: It was studied for two time intervals (6 or 24) h [50].

4.5. Characterization of silver nanoparticles

4.5.1. Uv-visible scanning

The bio-reduction of silver nitrate solution to silver nanoparticles was confirmed by UV–Vis spectroscopy. The sample was diluted with deionized water (1/10) and the highest absorbance (λmax) of AgNPs has been measured in the wavelength range from 300 to 600 nm to confirm the presence of specific Surface Plasmon Resonance (SPR) peak of AgNPs [51].

4.5.2. FTIR analysis

FTIR analysis was performed to find out possible functional groups responsible for the capping of silver nanoparticles. The suspension of AgNPs was centrifuged at 15000 rpm for 15 min. Then, the supernatant was discarded and 5 mL of deionized water was added to the pellet. The resulting suspension was poured into a watch glass and allowed to evaporate to obtain the powder of NPs. AgNPs were characterized by FTIR in the field extending from 400 to 4000 cm^{-1}. The dried sample was mixed with KBr (ratio 1:50) and pressed into discs using special press [52].

4.5.3. AFM analysis

AgNPs were first ultra-sonicated for 20 min and a drop of the sample was placed on a glass slide and was allowed to dry at 25 ^{0}C. The scan was performed by using an AFM apparatus [AFM Nanosurf Easyscan] [3,53].

4.5.4. Particle size and Zeta potential measurements

The mean particle size, polydispersity index (PDI), and zeta potential of prepared nanoparticles were determined by using DLS on a Zetasizer instrument at 25°C [51].

4.5.5. SEM analysis

The sample was prepared by dropping nanoparticle suspension on a glass slide and drying it at 25°C, then surface morphology examination was done by using Scanning Electron Microscope (SEM) (MIRA3 TESCAN, Czech Republic) at (SEM MAG = 100.00 K X) and (SEM HV = 5.00 K V) [3].

4.6 Stability study of the synthesized silver nanoparticles after 60 days

In order to evaluate the stability of the manufactured silver nanoparticles, its size and PDI were monitored at different time points 0, 10, 30, 45, and for 60 days by using DLS on a Zetasizer instrument at 25°C [13].

4.7. In vivo wound-healing study

4.7.1. Procedure for preparation of AgNPs Ointment

50 g of an ointment base was prepared by weighing 2.5 g of hard paraffin in a ceramic mortar and pestle. Then, 2.5 g of Cetostearyl alcohol, 2.5 g of Wool fat, 2.5 g of Propylene glycol, and 40 g of Yellow soft paraffin were added in descending order of their melting temperature, respectively. All the inactive ingredients were melted over a water bath with constant stirring and mixed homogeneously. Lastly, the ointment base was set away from a heat source and stirred until cool [54]. Silver nanoparticles were added to the ointment base to obtain a final concentration of 1% w/w, which was used for wound healing experiments. In addition, gentamicin sulfate ointment (0.1%) was used as a positive control.

4.7.2. Experimental animals

Twenty Wistar rats (150–200 g; 7 months old) were obtained from the Animal House Center of the Faculty of Pharmacy, Aleppo University. The animals were housed in aerated plastic cages (one rat/cage) and maintained under controlled room temperature and humidity with 12/12-hours light-dark cycle. The rats had free access to food and water. The protocol of this study was approved by the Ethics Committee of the Faculty of Pharmacy, Aleppo university, Syria (registration number: 3/I, 2022). All experiments and procedures used in this study were according to the established public health guidelines in Guide for Care and Use of Laboratory Animals (2011) [55].

4.7.3. Experimental Design

Rats were anesthetized by intraperitoneal injection of ketamine (90 mg/kg), then the dorsal lumbar fur of the rats was shaved, and two full-thickness skin wounds of 1.5 cm length were created by using a surgical blade [56]. Later, experimental rats were divided into four groups, each group consisting of five animals. The experimental group specifications are as follows;

- Group I (control): without treatment
- Group II (positive control): treated with a commercial ointment containing gentamycin 0.1%.
- Group III: treated with AgNPs ointment 1%.
- Group IV (negative control): treated with the ointment base only (without AgNPs).

4.7.4. The wound-healing period

The ointments were applied topically on rats once a day until reaching complete wound healing without any covering. Length of wound was measured on the 0th, 3rd, 6th, 9th, 12th, 15th, 18th, 21st, and 24th days, then it was compared with primary wound length [57]. Finally, healing times were determined for all experimental groups.

4.8. Statistical analysis:

All experiments were replicated as the mean ± standard deviation. Statistical analysis was made using the SPSS 23.00 analysis program, Differences in means values were examined using a one-way ANOVA, Tukey test as post-hoc tests, and differences were considered to be significant at $p < 0.05$.

Author contributions: Concept – M.A., W.A., A.K.; Design – M.A., W.A., A.K.; Supervision – M.A., W.A., A.K.; Resources – M.A., W.A., A.K.; Materials – W.A., A.K.; Data Collection and/or Processing – M.A.; Analysis and/or Interpretation – M.A., W.A., A.K.; Literature Search – M.A.; Writing – M.A.; Critical Reviews – M.A., W.A., A.K.

Conflict of interest statement: The authors declared no conflict of interest.

REFERENCES

[1] Kumar R, Ghoshal G, Jain A, Goyal M. Rapid Green synthesis of silver nanoparticles (AgNPs) using (Prunus persica) plants extract: Exploring its Antimicrobial and catalytic activities. J Nanomed Nanotechnol. 2017; 8(4): 1-8.
[2] Khattak A, Ahmad B, Rauf A, Bawazeer S, Farooq U, Ali J, Patel S, El-Sharkawy E, Ikram R, Linfang H. Green synthesis, characterisation and biological evaluation of plant-based silver nanoparticles using Quercus semecarpifolia Smith aqueous leaf extract. IET Nanobiotechnol. 2019; 13(1): 36–41. https://doi.org/10.1049/iet-nbt.2018.5063.
[3] Rashmi V, Sanjay KR, Green synthesis, characterization and bioactivity of plant-mediated silver nanoparticles using Decalepis hamiltonii root extract. IET Nanobiotechnol. 2017; 11(3): 247-254. https://doi.org/10.1049/iet-nbt.2016.0018.
[4] Chaudhuri SK, Chandela S, Malodia L. Plant mediated green synthesis of silver nanoparticles using Tecomella undulata leaf extract and their characterization. Nano Biomed Eng. 2016; 8(1):1–8. http://dx.doi.org/10.5101/nbe.v8i1.p1-8.
[5] Khan I, Saeed K, Khan I. Nanoparticles: Properties, applications and toxicities. Arab J Chem. 2019; 12(7): 908–931. https:// doi.org/10.1016/j.arabjc.2017.05.011.
[6] Bhaduri GA, Littlea R, Khomanec RB, Lokhandeb SU, Kulkarnic BD, Mendisd BG, Siller L. Green synthesis of silver nanoparticles using sunlight. J Photochem Photobiol A Chem. 2013; 258 (2013): 1–9. https://doi.org/10.1016/j.jphotochem.2013.02.015.
[7] Niska K, Zielinska E, Radomski MW, and Inkielewicz-Stepniak I. Metal nanoparticles in dermatology and cosmetology: Interactions with human skin cells. Chem Biol Interact. 2018; 295: 38–51. https://doi.org/10.1016/j.cbi.2017.06.018.
[8] Prabhu S, Poulose EK. Silver nanoparticles: mechanism of antimicrobial action, synthesis, medical applications, and toxicity effects. Int Nano Lett. 2012; 2(1): 1-10. https://doi.org/10.1186/2228-5326-2-32.
[9] Ren Y, Yang H, Wang T, Wang C. Bio-synthesis of silver nanoparticles with antibacterial activity. Mater Chem Phys. 2019; 235(2019): 121746. https://doi.org/10.1016/j.matchemphys.2019.121746.
[10] Panda SK, Sen S, Roy S, Moyez A. Synthesis of Colloidal silver nanoparticles by reducing aqueous AgNO3 using green reducing agents. Mater Today Proc. 2018; 5(3): 10054–10061. https://doi.org/10.1016/j.matpr.2017.10.206.
[11] Kulkarni N., Muddapur U. Biosynthesis of Metal Nanoparticles: A Review. Journal of Nanotechnology. 2014; (2014): 1-8. https://doi.org/10.1155/2014/510246.
[12] Gavade SJM, Nikam GH, Sabale SR, Dhabbe RS, Mulik GN, Tamhankar BV. Green synthesis of silver nanoparticles by using Acacia concinna fruit extract and their antibacterial activity. Nanosci Nanotechnol. 2015;9 (3):89–94.
[13] Jalab J, Abdelwahed W, Kitaz A, Al-kayali R. Green synthesis of silver nanoparticles using aqueous extract of Acacia cyanophylla and its antibacterial activity. Heliyon. 2021; 7(9): e08033. https://doi.org/10.1016/j.heliyon.2021.e08033.
[14] Koduru JR, Kailasa SK, Bhamore JR, Kim KH, Dutta T, Vellingiri K. Phytochemical-assisted synthetic approaches for silver nanoparticles antimicrobial applications: A review. Adv Colloid Interface Sci. 2018; 256: 326–339. https://doi.org/10.1016/j.cis.2018.03.001.
[15] Hajialyani M, Tewari D, Sobarzo-Sánchez E, Nabavi SM, Farzaei MH, Abdollahi M. Natural product-based nanomedicines for wound healing purposes: Therapeutic targets and drug delivery systems. Int J Nanomed. 2018; 13: 5023–5043. https://doi.org/10.2147/ijn.s174072.
[16] Dhapte V, Kadam S, Moghe A, Pokharkar V. Probing the wound healing potential of biogenic silver nanoparticles. J Wound Care. 2014; 23(9): 431–441. https://doi.org/10.12968/jowc.2014.23.9.431.
[17] Bhuvaneswari T, Thiyagarajan M, Geetha N, Venkatachalam P. Bioactive compound loaded stable silver nanoparticle synthesis from microwave irradiated aqueous extracellular leaf extracts of Naringi crenulata and its wound healing activity in experimental rat model. Acta Trop. 2014; 135: 55–61. https://doi.org/10.1016/j.actatropica.2014.03.009.
[18] Chandran SP, Chaudhary M, Pasricha R, Ahmad A, Sastry M. Synthesis of gold nanotriangles and silver nanoparticles using Aloe vera plant extract. Biotechnol Prog. 2006; 22(2): 577–583. https://doi.org/10.1021/bp0501423.
[19] Jurjus A, Hourani R, Daouk H, Youssef L, Bou-Khalil P, Haidar H, Saade N. Effect of denervation on burn wound healing. Ann Burns and Fire Disasters. 2018; 31(4): 278.
[20] Bozorgi M, Memariani Z, Mobli M, Salehi Surmaghi MH, Shams-Ardekani MR, Rahimi R. Five Pistacia species (P.

vera, P. atlantica, P. terebinthus, P. khinjuk, and P. lentiscus): a review of their traditional uses, phytochemistry, and pharmacology. Sci World J. 2013; 2013: 219815. https://doi.org/10.1155/2013/219815.
[21] Saleh AL, Fuad AR, Jehad A, Saleh AN, Khaled Q. Separation and identification of phenolics and flavonoids from wild Pistacia palaestina extract and its antioxidant activity. J Med Plants Res. 2020; 14(7): 317–325. https://doi.org/10.5897/JMPR2020.6969.
[22] Al-Mustafa A. Phytochemical analysis, antioxidant and anti-acetylcholinesterase activities of Jordanian Pistacia palaestina Bios leaves extract. Trop J Nat Prod Res. 2021; 5(9):1619-1625. http://www.doi.org/10.26538/tjnpr/v5i9.15
[23] Naghmachi M, Raissi A, Baziyar P, Homayoonfar F, Amirmahani F, Danaei M. Green synthesis of silver nanoparticles (AgNPs) by Pistacia terebinthus extract: Comprehensive evaluation of antimicrobial, antioxidant and anticancer effects. Biochem Biophys Res Commun. 2022; 608: 163-169. https://doi.org/10.1016/j.bbrc.2022.04.003.
[24] Golabiazar R, Othman KI, Khalid KM, Maruf DH, Aulla SM, Yusif PA. Green synthesis, characterization, and investigation antibacterial activity of silver nanoparticles using Pistacia atlantica leaf extract. Bionanoscience. 2019; 9(2): 323–333. https://doi.org/10.1007/s12668-019-0606-z.
[25] El-Chaghaby GA, Ahmad AF. Biosynthesis of silver nanoparticles using Pistacia lentiscus leaves extract and investigation of their antimicrobial effect. Orient J Chem. 2011; 27(3): 929–936.
[26] Husain S, Afreen S, Yasin D, Afzal B, Fatma T. Cyanobacteria as a bioreactor for synthesis of silver nanoparticles-an effect of different reaction conditions on the size of nanoparticles and their dye decolorization ability. J Microbiol Methods. 2019; 162: 77–82. https://doi.org/10.1016/j.mimet.2019.05.011.
[27] Lade BD, Shanware AS. Phytonanofabrication: Methodology and Factors Affecting Biosynthesis of Nanoparticles. Smart Nanosystems for Biomedicine, Optoelectronics and Catalysis. IntechOpen 2020; 1–17. http://dx.doi.org/10.5772/intechopen.90918.
[28] Ahmad B, Shireen F, Rauf A, Shariati A, Bashir MA, Patel S, Zhang H. Phyto-fabrication, purification, characterisation, optimisation, and biological competence of nano-silver. IET Nanobiotechnol. 2021; 15(1):1–18. https://doi.org/10.1049/nbt2.12007.
[29] Khiya Z, Oualcadi Y, Mourid EH, Tagnaout I, Berrekhis F, Zair T, El Hilali F. Evaluation antioxidant and antibacterial activities of silver nanoparticles synthesized by aqueous extract of Pistacia atlantica. Res Chem Intermed. 2021; 47(8): 3131–3144. https://doi.org/10.1007/s11164-021-04468-w
[30] Essghaier B, Ben Khedher G, Hannachi H, Dridi R, Zid MF, Chaffei C. Green synthesis of silver nanoparticles using mixed leaves aqueous extract of wild olive and pistachio: characterization, antioxidant, antimicrobial and effect on virulence factors of Candida. Arch Microbiol. 2022; 204(4): 1-13. https://doi.org/10.1007/s00203-022-02810-3
[31] Rivera-Rangel RD, González-Muñoz MP, Avila-Rodriguez M, Razo-LazcanoTA, Solans C. Green synthesis of silver nanoparticles in oil-in-water microemulsion and nano-emulsion using geranium leaf aqueous extract as a reducing agent. Colloids Surf A Physicochem Eng Asp. 2018; 536: 60–67. https://doi.org/10.1016/j.colsurfa.2017.07.051
[32] Barberia-Roque L, Gámez-Espinosa E, Viera M, Bellotti N. Assessment of three plant extracts to obtain silver nanoparticles as alternative additives to control biodeterioration of coatings. Int Biodeterior Biodegrad. 2019; 141: 52–61. https://doi.org/10.1016/j.ibiod.2018.06.011.
[33] Sherin L, Sohail A, Amjad UES, Mustafa M, Jabeen R, Ul-Hamid A. Facile green synthesis of silver nanoparticles using Terminalia bellerica kernel extract for catalytic reduction of anthropogenic water pollutants. Colloids Interface Sci Commun. 2020; 37: 100276. https://doi.org/10.1016/j.colcom.2020.100276.
[34] Khan SA, Shahid S, Lee CS. Green synthesis of gold and silver nanoparticles using leaf extract of clerodendrum inerme; characterization, antimicrobial, and antioxidant activities. Biomolecules. 2020; 10(6): 100276. https://doi.org/10.3390/biom10060835.
[35] Umoren SA, Obot IP, Gasem ZM. Green synthesis and characterization of silver nanoparticles using red apple (Malus domestica) fruit extract at room temperature. J Mater Environ Sci. 2014; 5(3): 907-914.
[36] Swamy MK, Akhtar MS, Mohanty SK, Sinniah UR. Synthesis and characterization of silver nanoparticles using fruit extract of Momordica cymbalaria and assessment of their in vitro antimicrobial, antioxidant and cytotoxicity activities. Spectrochim Acta A: Mol Biomol Spectrosc. 2015; 151: 939-944. https://doi.org/10.1016/j.saa.2015.07.009.
[37] Xu S, Arnsdorf MF. Calibration of the scanning (atomic) force microscope with gold particles. J Microsc. 1994; 173(3): 199-210. https://doi.org/10.1111/j.1365-2818.1994.tb03442.x.
[38] Ravichandran V, Vasanthi S, Shalini S, Shah SAA, Harish R. Green synthesis of silver nanoparticles using Atrocarpus altilis leaf extract and the study of their antimicrobial and antioxidant activity. Mater Lett. 2016; 180: 264–267. https://doi.org/10.1016/j.matlet.2016.05.172.
[39] Honary S, Zahir F. Effect of Zeta Potential on the Properties of Nano-Drug Delivery Systems - A Review (Part 1). Trop J Pharm Res. 2013; 12(2), 255–264. http://dx.doi.org/10.4314/tjpr.v12i2.19.
[40] Pinto VV, Ferreira MJ, Silva R, Santos HA, Silva F, Pereira CM. Long time effect on the stability of silver nanoparticles in aqueous medium: Effect of the synthesis and storage conditions. Colloids Surfaces A Physicochem Eng Asp. 2010; 364(1–3): 19–25. https://doi.org/10.1016/j.colsurfa.2010.04.015.
[41] Al-Shmgani HSA, Mohammed WH, Sulaiman GM, Saadoon AH. Biosynthesis of silver nanoparticles from Catharanthus roseus leaf extract and assessing their antioxidant, antimicrobial, and wound-healing activities. Artif Cells Nanomed Biotechnol. 2017; 45(6): 1234–1240. http://dx.doi.org/10.1080/21691401.2016.1220950.

[42] Naraginti S, Kumari PL, Das RK, Sivakumar A, Patil SH, Andhalkar VV. Amelioration of excision wounds by topical application of green synthesized, formulated silver and gold nanoparticles in albino Wistar rats. Mater Sci Eng C. 2016; 62: 293–300. http://dx.doi.org/10.1016/j.msec.2016.01.069.
[43] Liu X, Lee PY, Ho CM, et al. Silver nanoparticles mediate differential responses in keratinocytes and fibroblasts during skin wound healing. Chem Med Chem. 2010; 5(3): 468–475. https://doi.org/10.1002/cmdc.200900502
[44] Gunasekaran T, Nigusse T, Dhanaraju MD. Silver nanoparticles as real topical bullets for wound healing. J Am Coll Clin Wound Spec. 2011; 3(4): 82–96. https://doi.org/10.1016%2Fj.jcws.2012.05.001.
[45] Adawia K, Yaser AM, Molham Al-N. Comparison between Total Phenolic and Flavonoid Contents and Antidiabetic Activities of Different Parts of Capparis spinosa L. growing in Aleppo, Syria. Int J Pharmacogn Phytochem Res. 2020; 12(3): 143-152. http://dx.doi.org/10.25258/phyto.12.3.4.
[46] Aslany S, Tafvizi F, Naseh V. Characterization and evaluation of cytotoxic and apoptotic effects of green synthesis of silver nanoparticles using Artemisia Ciniformis on human gastric adenocarcinoma. Mater Today Commun. 2020; 24(8): 101011. http://dx.doi.org/10.1016/j.mtcomm.2020.101011.
[47] Hasnain MS, Javed MN, Alam MS, Rishishwara P, Rishishwara S, Ali S, Beg S. Purple heart plant leaves extract mediated silver nanoparticle synthesis: Optimization by Box-Behnken design. Mater Sci Eng C. 2019; 99: 1105–1114. https://doi.org/10.1016/j.msec.2019.02.061.
[48] Singh M, Sinha I, Mandal RK. Role of pH in the green synthesis of silver nanoparticles. Mate. Lett. 2009; 63(3–4): 425–427. https://doi.org/10.1016/j.matlet.2008.10.067.
[49] Seifipour R, Nozari M, Pishkar L. Green Synthesis of Silver Nanoparticles using Tragopogon Collinus Leaf Extract and Study of Their Antibacterial Effects. J Inorg Organomet Polym and Materials. 2020; 30(8): 2926–2936. https://doi.org/10.1007/s10904-020-01441-9.
[50] Sharma K, Guleria S, Razdan VK. Green synthesis of silver nanoparticles using Ocimum gratissimum leaf extract: characterization, antimicrobial activity and toxicity analysis. J Plant Biochem Biotechnol 2020; 29(2): 213–224. https://doi.org/10.1007/s13562-019-00522-2.
[51] Malaikozhundan B, Vijayakumar S, Vaseeharan B, Jenifer AA, Chitra P, Prabhu NM, Kannapiran E. Two potential uses for silver nanoparticles coated with Solanum nigrum unripe fruit extract: Biofilm inhibition and photodegradation of dye effluent. Microb Pathog. 2017; 111: 316-324. https://doi.org/10.1016/j.micpath.2017.08.039.
[52] Singh A, Jain D, Upadhyay MK, Khandelwal N, Verma HN. Green synthesis of silver nanoparticles using Argemone Mexicana leaf extract and evaluation of their antimicrobial activities. Dig J Nanomater Biostruct. 2010; 5(2): 483–489.
[53] Priya RS, Geetha D, Ramesh PS. Antioxidant activity of chemically synthesized AgNPs and biosynthesized Pongamia pinnata leaf extract mediated AgNPs – A comparative study. Ecotoxicol Environ Saf. 2016; 134(2): 308–318. https://doi.org/10.1016/j.ecoenv.2015.07.037.
[54] Kamarapu P, Sailakshmi P. Formulation and evaluation of anti-microbial polyherbal ointment. J Bioeng Biomed. Sci. 2015; 5(2): 63–68. http://dx.doi.org/10.4172/2155-9538.1000154.
[55] National Research Council (US) Committee for the Update of the Guide for the Care and Use of Laboratory Animals. Guide for the Care and Use of Laboratory Animals. 8th edition. Washington (DC): National Academies Press (US) 2011. https://doi.org/10.17226/12910.
[56] Eyo JE, Uzoibiam BO, Ogbanya KC, Nnaji TO. Comparative evaluation of wound healing effects of Ocimum gratissimum, Vernonia amygdaline and Zingiber officinalis extracts on incision wound model in rats. Pharmacologyonline. 2014; 3(September): 44–50.
[57] Venkatachalam P, Sangeetha P, Geetha N, Sahi SV. Phytofabrication of bioactive molecules encapsulated metallic silver nanoparticles from Cucumis sativus L. and its enhanced wound healing potential in rat model. J Nanomater 2015; (2015): 1-9. http://dx.doi.org/10.1155/2015/753193.